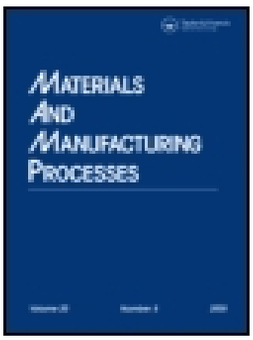

Taylor & Francis
Taylor & Francis Group

Materials and Manufacturing Processes

ISSN: (Print) (Online) Journal homepage: https://www.tandfonline.com/loi/lmmp20

Manufacturing and forging issues encountered while upscaling 1.3C30Mn10Al-austenitic and 0.65C12Mn-duplex low-density steels

Idurre Kaltzakorta, Teresa Gutierrez, Roberto Elvira, Pello Jimbert & Teresa Guraya

To cite this article: Idurre Kaltzakorta, Teresa Gutierrez, Roberto Elvira, Pello Jimbert & Teresa Guraya (2021): Manufacturing and forging issues encountered while upscaling 1.3C30Mn10Al-austenitic and 0.65C12Mn-duplex low-density steels, Materials and Manufacturing Processes, DOI: 10.1080/10426914.2021.1944192

To link to this article: https://doi.org/10.1080/10426914.2021.1944192

Published online: 05 Jul 2021.

MATERIALS AND MANUFACTURING PROCESSES
https://doi.org/10.1080/10426914.2021.1944192

Manufacturing and forging issues encountered while upscaling 1.3C30Mn10Al-austenitic and 0.65C12Mn-duplex low-density steels

Idurre Kaltzakorta[a], Teresa Gutierrez[a], Roberto Elvira[b], Pello Jimbert[c], and Teresa Guraya[c]

[a]TECNALIA, Basque Research and Technology Alliance (BRTA), Parque Científico Y Tecnológico De Bizkaia, Derio, Spain; [b]Sidenor I+D, Barrio Ugarte S/n, Basauri, Spain; [c]Faculty of Engineering in Bilbao, University of the Basque Country UPV/EHU, Paseo Rafael Moreno "Pitxitxi" 3, Bilbao, Spain

ABSTRACT

Difficulties found when manufacturing and forging two low density steels in different scales are described in this work. Austenitic and duplex low-density steels have attracted a lot of interest due to their good combination of mechanical properties and density reduction. In this work, the fabrication of 1.3 C30Mn10Al austenitic low-density steel and 0.65 C12Mn10Al duplex low-density steel have been studied. The scaling up of the manufacturing process from 1 Kg to 35 Kg ingots of both materials and the subsequent hot forging of the ingots is described, showing the difficulties encountered during the production and transformation of these steels. Only the small ingots were successfully forged, but not the larger ones, showing the important differences in the forging properties depending on the geometry and dimensions of the final part to be forged, and the homogenization temperatures. The possible causes of this scale dependence are proposed from the experimental results obtained, as well as from the hot axial compression tests and the thermodynamic simulations carried out.

ARTICLE HISTORY
Received 12 February 2021
Accepted 1 June 2021

KEYWORDS
Low-density steels; hot forging; fecmnal; Gleeble

Introduction

To comply with strict fuel economy and CO_2 emission reduction policies, the automotive industry is working on reducing the weight of cars, but without penalizing passenger safety (a 100Kg reduction in vehicle weigh means about 7.5–12.5g less CO_2 emissions per kilometer).[1] To this end, different strategies are being adopted, such as the use of HSS to minimize thicknesses, the redesign of components to eliminate unnecessary material, and the reduction of density of the material used. In this last approach, even if steel is strongly competing with other lighter materials, such as Al, Mg, etc, steel has the advantage of being the most environmentally friendly material, due to its recyclability. In the literature, most publications on low-density steels refer to vehicle structural parts, [2,3,4] while nearly no publications focus on forged components.

Drop forging, or hot forging, is a hot metal working process in which the metal is heated to the appropriate or required temperature to achieve the plastic deformation necessary to obtain the final shape of the work piece in solid state by compressive forces applied using dies and tools.[5] Among all transformation processes, forging occupies a special place because it allows parts with superior mechanical properties to be obtained with a minimum waste of material . Hot forging takes place at temperatures above recrystallization. Forging usually requires relatively expensive tooling, but this is not a disadvantage when a large number of parts have to be produced or when forging is the only transformation process that can obtain the required final mechanical properties; in these cases forging process is an economically competitive transformation process.[6]

Low-density steels are Fe-C-Mn-Al steels to which a relevant quantity of aluminum is added to decrease the overall density of the steel. The addition of 1% Aluminum leads to a reduction in density of 1.3% [7], but at the same time, also leads to a reduction in Young's modulus of 2%.[2] Taking into account the chemical composition (% by weight) of low-density steels, they can be differentiated into three groups[6]: ferritic steels (%Mn<8, 5<%Al<8, %C < 0.03), austenitic steels (15<%Mn<30, 8<%Al<12, 0.5<%C < 2), and duplex steels (5<%Mn<30, 3<%Al<10, 0.1<%C < 0.7). In recent years, numerous works[2,3,47,8,9,10,11,12,13,14,15,16] have been reported concerning the synthesis and mechanical behavior of low-density steels. Most of the publications are aimed at the laboratory scale and at vehicle structural parts in order to reduce the weight of car parts without penalizing the security of the users.

The low-density steels of greatest industrial interest are low-density austenitic steels because of their greater strength, ductility and density reduction potential,[2,17] but because of their composition they are the steels with the greatest manufacturing problems. Duplex steels are the next option of interest, due to their mechanical characteristics and the lower content of the alloying elements in their compositions, which in theory facilitate their manufacture. In addition to the manufacturing drawbacks, the literature also describes the processing drawbacks of low-density steels, [2,7,18] which hinders the commercialization of these new, lighter steels. The literature describes the hot deformation behavior of low-density steels, [19,20,21,22] and relates the dependence of the dynamic recrystallization of the experimental steel on the deformation temperature and strain rate, but does not define the scale dependence of the

CONTACT Idurre Kaltzakorta Idurre.Kaltzakorta@tecnalia.com TECNALIA, Basque Research and Technology Alliance (BRTA), Parque Científico Y Tecnológico De Bizkaia, C/Astondoa, Edificio 700, Derio, 48160, Spain

Table 1. Theoretical compositions of the two low-density steels.

STEEL	TARGET COMPOSITION (wt%)
DUPLEX	0.65C 12Mn 10Al
AUSTENITIC	1.3 C 30Mn 10Al

forging process. The present work starts using a lab scale, high purity, levitation furnace (1Kg), in order to study the casting capability of two types of low-density steels (an austenitic steel with composition of 1.3C30Mn10Al and a duplex steel with composition 0.65C12Mn10Al), and subsequent forging of the ingots. The idea was to upscale the process, going through a 5Kg induction vacuum furnace and finishing the study in a 35Kg vacuum furnace of a steelmaker. Different precautions were taken at the different scales to minimize problems in the manufacturing process. As all the ingots manufactured here are intended for hot forging, and with the idea of designing the best procedure for this forging process, the behavior of the materials in the hot forging temperature range was studied by means of thermodynamic simulations (withThermoCalc software) and hot ductility tests (with a Gleeble machine). From the results obtained, some recommendations on manufacturing and transformation processes are given for future research in the field of low-density steels for hot forging.

Materials and methods

Two different types of low-density steels were selected for this research, one duplex-austenitic and one austenitic low-density steel. The theoretical compositions of the two grades vary in carbon content and the alloying elements manganese and aluminum, as summarized in Table 1.

Materials production

With the purpose of making a scaling study, ingots of 1 Kg, 5 Kg and 35 Kg were produced in different furnaces in order to study the manufacturing upscale of these steels.

1Kg ingots produced in a levitation furnace

To obtain the selected duplex and austenitic steels, a levitation furnace working under vacuum and argon atmosphere was used. The raw materials used were iron (99.9+%), graphite (99+%), manganese (99+%) and pure aluminum (99%+). Cylindrical ingots of approximately 1 kg were cast for both compositions (Figure 1). The levitation furnace has the advantage of working in an inert atmosphere, which avoids the risk of material contamination and thus produces a pure and reproducible melt and also allows re-melting. In order to guaranty a homogeneous distribution of the composition all over the ingot, two re-melts were performed.•

Figure 1. 1 Kg ingot casted in the levitation vacuum furnace.

5Kg ingots produced in an induction furnace

To scale up the manufacturing process of these steels, a Consarc Vacuum Induction Melting and Casting Furnace was selected for the study. To carry out the casting, a procedure consisting of melting electrolytic iron (99.85% Fe) in the vacuum oven was followed and, once melted, introducing a partial pressure of argon before proceeding to add the necessary alloying elements through the loading chamber located at the top of the melting chamber in the following formats: pure aluminum in form of pieces, pure manganese in form of flakes and carbon in the form of graphite powder. When the dissolution of the alloying elements in the iron is assumed, the induction furnace is switched off to stop heating and the contents of the crucible are poured into the adjacent mold. After ensuring solidification, the argon is removed from the chamber and the vacuum is broken.Table 3 The casting of both steels was quite good, no excessive slag was formed, and all the added material seemed to be well incorporated (Figure 2). After machining to remove the squeeze, the approximate dimensions of the ingots were: 75x75x60mm.

35Kg ingots produced in an induction furnace

To further scale up the steelmaking process, the next step was a 35 Kg induction furnace. The ingots were produced under conditions similar to the industrial process. A VCM030 Induction Vacuum Melting & Casting Furnace was used. As

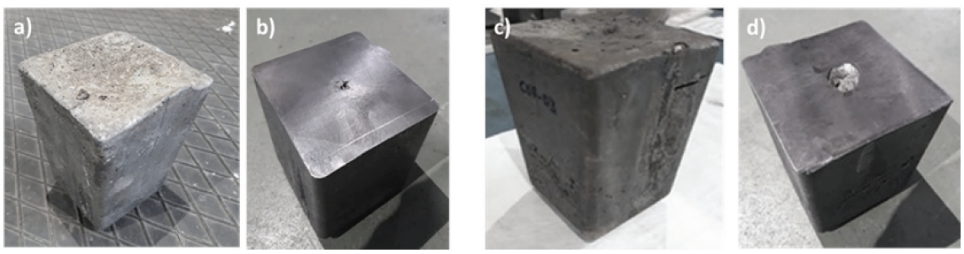

Figure 2. 5 Kg ingots of the (a, b) duplex and (c, d) austenitic low-density steels. (a, c) when removed from the mold. (b, d) after partially machining.

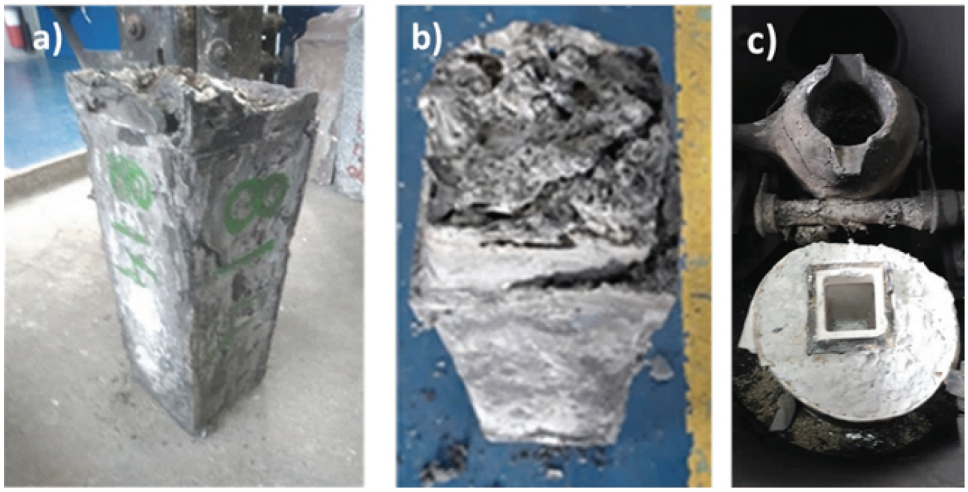

Figure 3. 35 Kg ingots manufactured of (a) austenitic low-density steel and (b)duplex low-density steel. c) Mold isolated with Vermiculite.

raw material, graphite powder, Ø12 aluminum steel bars, ferromanganese (packed in aluminum cans), Ø60 cast iron bars and Ø90 electrolytic iron bars were used, stacked in the crucible to place the ferromagnetic material up to the middle, where the induction coil has the highest action. Moreover, considering the amount of manganese and aluminum to be added, a remarkable heterogeneity in the structure of the casting was expected, as well as stresses during solidification, which could affect the subsequent forging of the ingots. Consequently, for these castings, several actions were taken to reduce possible thermal stresses during cooling. The mold was insulated with a thermal insulator (Vermiculite) to reduce the solidification rate on the ingot surface and match the solidification rate inside the ingot. In addition, the metal load of the ingot mold was increased to shift the segregation to the top and to obtain a structure as homogeneous as possible. Despite all the precautions taken, the appearance of the 35Kg ingots showed evidence of casting problems (Figure 3), It has been reported[2] that when a large amount of aluminum is used as an alloying element, intense chemical reactions can occur, leading to deviations from the desired chemical compositions and can also become a sign of poor steel quality. In this case, the low-density austenitic ingot showed surface cracks and both the austenitic and the duplex ingot showed a high amount of slag, which due to the vacuum furnace could not be removed, confirming the problems during manufacturing of these steels on larger scales.

Chemical composition analysis

Two different analytical techniques were used to analyze the chemical composition of the cast alloys. Aluminum and manganese contents were calculated using ICP-OES on a THERMO-ICAP 7400 DUO Plasma Emission Spectrometer. A LECO CS-400 carbon sulfur analyzer was used to analyze the C content after sample combustion.

Microstructural analysis and mechanical tests

Microstructural characterization was carried out following the traditional method. The samples were sectioned, mechanically grinded and polished followed by etching with Nital solution. The microstructure characterization was studied using optical microscopy under a Leica DM400 and a LEICA DMI5000M and Scanning Electron Microscopy with a Carl Zeiss EVO-40 equipped with an energy dispersive spectrometer (EDS). A 5500 R-Instron machine, was employed to perform the mechanical tests.

Forge of the ingots

High alloy steels require slow heating and cooling steps to avoid the formation of mechanical stresses due to high thermal gradients. For 1Kg ingots the cross-section is about 500mm^2, while for 35Kg ingots it is 10,000mm^2, 20 times larger, and the mass to be heated is 40 times greater. To achieve the forging of the 35Kg ingots, additional precautions were taken during the process, slower heating to avoid thermal stresses (5°C/min until 800°C, 10°C/min until 1100°C and 2hours of homogenization). In the case of 1Kg and 5Kg scales, all the ingots were heated up to 1100°C with a heating rate of 10°C/min in a gas furnace and 1 hour of homogenization was applied for the 5Kg ingots and 15minutes for the 1Kg ingots and reheated as soon as the temperature dropped below 900°C. In all cases, a digital pyrometer (Land Ametek Cyclops Series-L) was used to monitor the ingot temperature. Drop hot forging with manual control was applied in all cases.

Hot working tests

For the hot working tests, a Geeble-3800 C thermo-mechanical simulator was used to perform axial compression tests and to study the hot ductility of these steels.

To define the test temperatures, simulations were performed with ThermoCalc in order to find the temperature window in which only the austenite and ferrite phases are

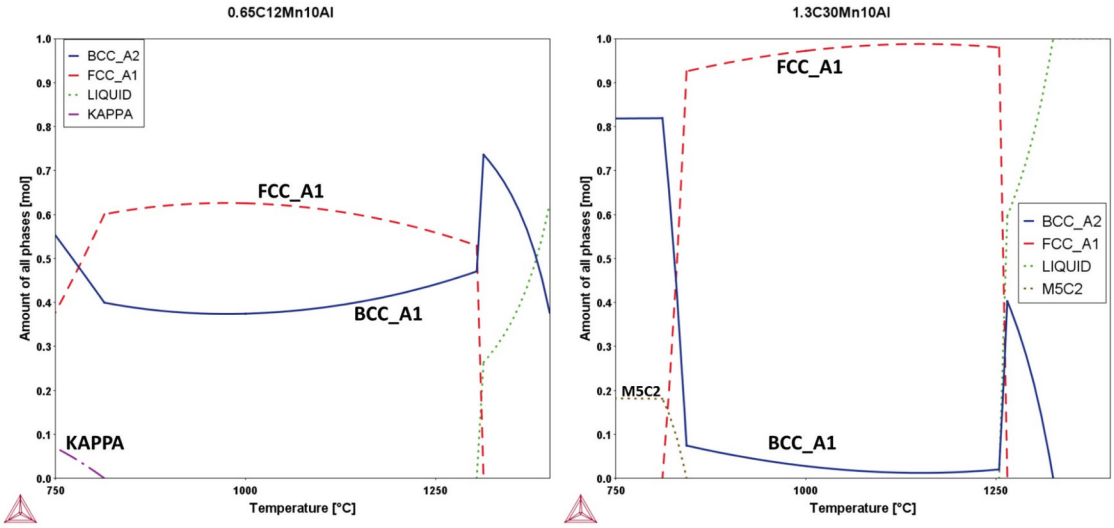

Figure 4. ThermoCalc phase diagrams of the theoretical compositions of the (a) austenite based duplex steel and (b), austenitic steel.

Table 3. Mechanical tests results for the forged low-density steels after heating up to 1150°C followed by AC-air cooling, or WQ-water quenching.

Steel	Heat Treatment at 1150°C	Yield Strength (MPa)	Tensile Strength (MPa)	Total Elongation (A30) (%)
AUSTENITIC 1 Kg	AC	1090	1141	37
DUPLEX 1 Kg	WQ	720	855	22.1
DUPLEX 5 Kg	WQ	565	772	27.2
DUPLEX 5 Kg	AC	679	823	19.8

formed. From the phase diagrams shown in Figure 4, temperatures in the range of 900–1100°C were selected. Strain rate conditions of 0.1, 1 and $10s^{-1}$ were selected as usual conditions in hot working processes. Due to the poor machinability of these steels in the as-cast condition, square prismatic specimens of 10x10x15 mm were machined for the axial compression tests instead of the typical 10mm diameter and 15 mm height cylinders. A tantalum foil was used between each anvil and the specimen to reduce friction. The specimens were heated to the target temperature at a rate of 3°C/s and held at that temperature for 1 minute before being subjected to 0.8% (axial) and 1% (planar) compression.

Table 2. Real compositions of the two low-density steels produced at different scales and the deviation of each composition from the target. The theoretical density calculated with the thermoCalc software is also provided.

Ingot Size	Low Density Steel	Real Composition (% wt)	%C	% Mn	% Al	Density (g/cm[3])
1 Kg	DUPLEX	0.66 C 11.4Mn 9.9Al	−1.5	−5	−1	6.85
	AUSTENITIC	1.3C 29.6Mn 9.9Al	0	−1.3	−1	6.77
5 Kg	DUPLEX	0.55 C 11.8Mn 8.6Al	−15.4	−1.7	−14	6.96
	AUSTENITIC	1.1 C 29.8Mn 9.6Al	−15.3	−0.7	−4	6.79
35 Kg	DUPLEX	0.68 C 13.4Mn 11.5Al	−4.6	11.7	15	6.7
	AUSTENITIC	1.3C 24.7Mn 12.7Al	0	17.7	27	6.56

Results and discussion

Many new problems arise in steel making due to the large quantity of aluminum in low density steels.[2] Aluminum is a good deoxidizer, however, when a large quantity of aluminum is used as an alloying element, intense chemical reactions can occur, whereby the large number of alloying elements and the size of the cast ingots lead to deviations from the intended design. Table 2 summarizes the values obtained for each alloy in the different ingot sizes and their deviations from the target values. Elements such as manganese and aluminum with lower melting temperature and higher vapor pressure compared to iron, respectively, make it difficult to control the addition to molten steel and keep the composition close to the target during casting process. This deviation is greater the larger the scale of the casting. *As for the significant deviations obtained for the cast steels, new ThermoCalc simulations (*Figure. 5*) were performed to confirm that the temperature range selected for the hot work tests remains within the domain where only austenite and ferrite phases exist.*

Forge of the ingots

It was previously stated that the forging operation was performed with a mechanical hammer (drop forging) at 1100° Cand reheating the ingots when temperature dropped below 900°C.The forging of the two 1Kg ingots was carried out with an average reduction of 50–60% of the cross-section with no noticeable problems*(*Figure. 6(a)*)*. The 5 Kg ingots showed different behavior during forging. The duplex steel was successfully forged in bar form, but the austenitic ingot burst and could not be forged correctly (Figure 6(b,c)*)*. The problem in forging the 5Kg low-density austenitic steel can be attributed to the higher stress levels required during the process as a result of the higher amount of alloying elements. To achieve the forging of the 35Kg ingots, additional precautions were taken during the process, slower heating to avoid thermal stresses*(5°C/*min until 800°*C, 10°C/*min until 1100°Cand 2hours of homogenization) and continuous reheating. In the

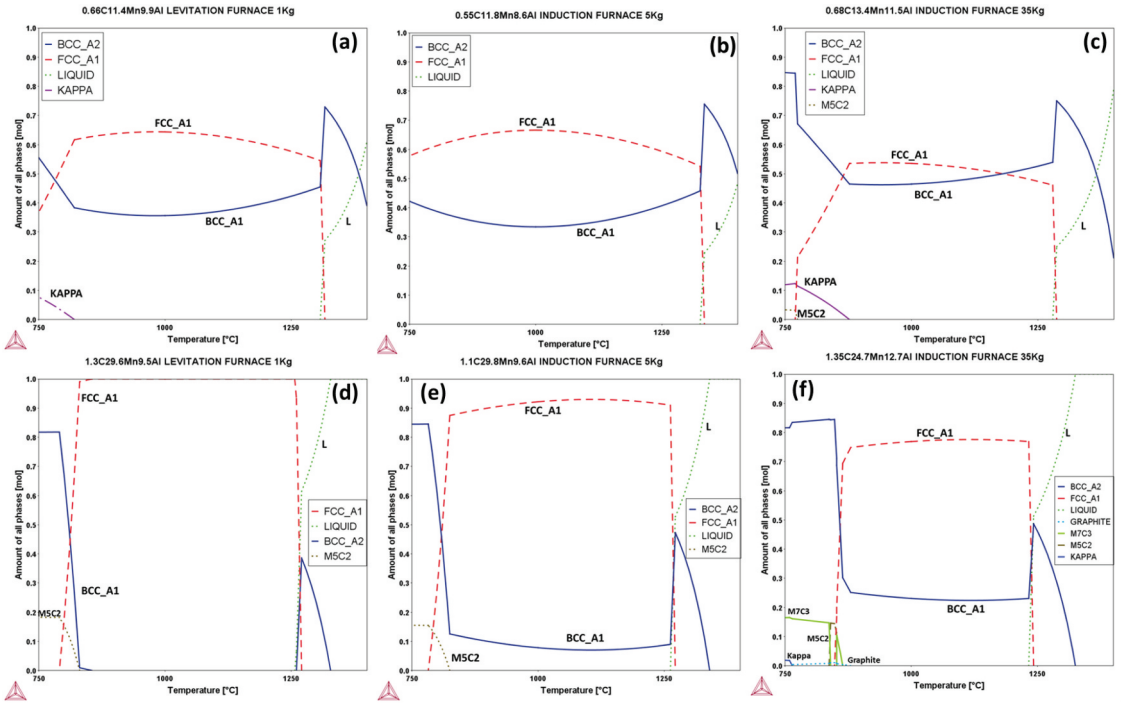

Figure 5. ThermoCalc phase diagrams of the final compositions of the: (a) 1 Kg, (b) 5 Kg and (c) 35 Kg duplex steels, and (d)1 Kg, (e) 5 Kg and (f) 35 Kg austenitic steel.

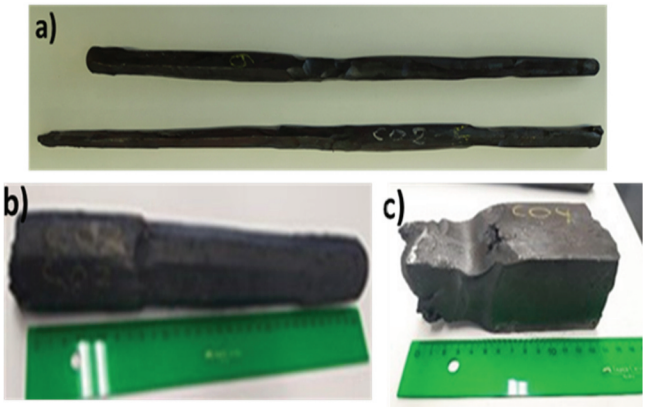

Figure 6. Forged ingots. (a) 1 Kg of austenitic and duplex low-density steels, (b) 5 Kg duplex low-density steel, and (c) 5 Kg austenitic low-density steel burst.

case of low-density duplex steel, after a few forging blows, two deep cracks emerged transverse to its axis*(Figure 7(a)),* so it was decided to suspend forging. The cracks became more visible and larger during cooling Figure (7b).In the case of austenitic low-density steel, considering the surface appearance of the ingot, it was quite clear that forging was going to be a problem, however it was decided to continue with the forge and as expected, the ingot broke at the first blow of the forge (Figure 7(c)). The ingot exhibited great resistance to hot deformation as well as high brittleness. These materials are extremely hard in hot condition and they behave like ceramic materials leading under compression stresses to brittle fractures without relevant deformation. As it is shown in Figure 7 (d), fractures are almost flat and in the parallel plane to the compression direction. Fracture seems to follow grain bounderies (Figure 7(f)) The different pieces (Figure 7(e)) showed phase heterogeneity of the ingot.

*When handling the heated austenitic parts, it was observed that their temperature dropped very quickly.*It was decided to perform Thermal Conductivity calculations using JMatPro® software. The thermal Conductivity of the six compositions used during the investigation was calculated and the thermal conductivity of 27MC5 steel, a common forging steel used for automotive components, was also calculated for comparison purposes. At 1000°C, *the thermal conductivity of the 35 Kg Austenitic composition was 40% higher, and the 35 Kg duplex composition was a 21% higher than the thermal conductivity of the 27MC5 steel at the same temperature. The high thermal conductivity of these steels combined with the larger ingot size of the 5Kg and 35Kg,could also affect their hot forging.*

Hot ductility tests

Since the forging of the 5Kg austenitic steel was unsuccessful, it was decided to perform the hot ductility test on all the larger ingots, i.e. the 5Kg and the 35Kg duplex and austenitic low-density steel ingots, in order to study the behavior of these materials at hot forming temperatures.

During the hot deformation process of most metallic materials, changes in the true stress-true strain curve come mainly from changes in the contribution of strain hardening and dynamic recovery and dynamic recrystallization. From the starting point of the curve, strain hardening progresses to a maximum stress value that corresponds to the maximum value of the deformation *(Ɛpeak).* After that point, the curves show a continous decrease in stress or under some conditions reach a steady sate (ie, a constant value) of stress. The steady state can occur at that maximum stress value on the curve or

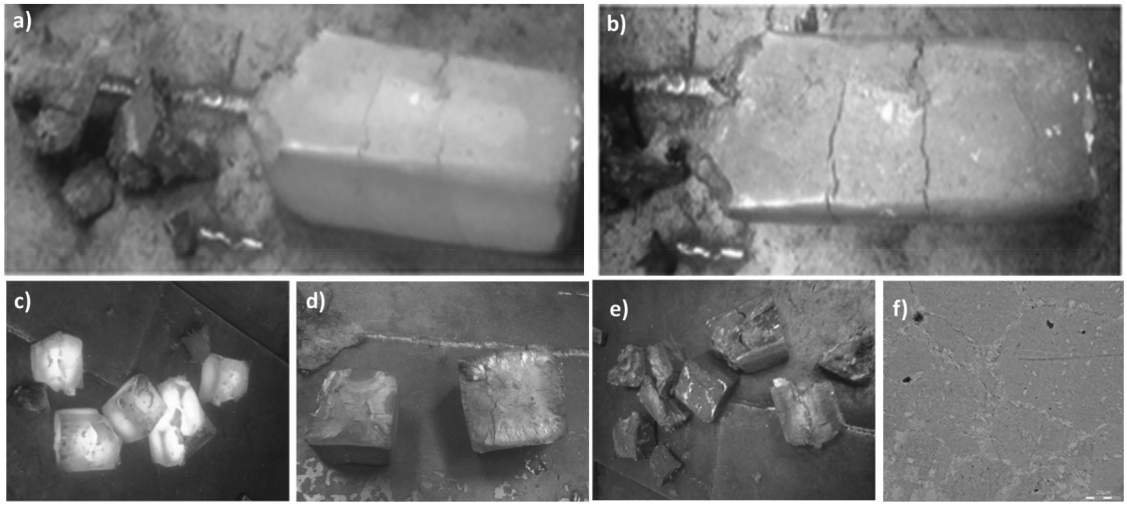

Figure 7. 35 kg ingots after forging process. (a)and (b) duplex low-density steel cracked ingot, (c) (d) and (e) austenitic low-density steel broken in pieces. (f) O. M. micrograph showing a crack propagating across grain boundaries in the austentic low density steel.

after a partial softening of the material. When the first case occurs, the material is recovered only by recovery mechanisms, whereas when softening occurs, it is related to additional recrystallization mechanisms. Hot working stress is, above all, sensitive to temperature and strain rate; for most materials, the higher the temperature and the lower the strain rate, the lower the stress. Figure 8 shows the flow curves obtained for the specimens extracted from the 5 Kg ingot of the duplex steel. All curves are as expected; the initial strain hardening of the material is higher for combinations of higher strain rates and lower temperatures. The values of Ɛpeak, the minimum strain required to initiate recovery mechanisms, move to higher values as the strain rate increases. In tests performed at the highest strain rate, the Ɛpeak value is significantly higher, i.e. at 1000°C more than double the maximum values observed at the lowest strain rate. After passing this point, the material starts a continuous softening. The activation of the dynamic of recovery and recrystallization mechanisms, results in a stress reduction of approximately 20% compared to the maximum stress values at the deformation peak. The curves of the samples tested at the intermediate strain rate, show fluctuations due to instabilities during compression. Samples tested at the lowest strain rate reach a steady state at strain values twice the maximum value. Figure 9 shows the flow curves obtained for the specimens extracted from the 5 Kg ingot of the austenitic steel. For this material, a third temperature of 1100°C was also tested. Compared to the curves obtained for the duplex steel produced at the same ingot scale (Figure 8), all the characteristics are quite comparable except for the strength value, which is remarkably higher for the austenitic steel when comparing the same test conditions. The maximum value of 360 MPa obtained for the duplex steel when tested at the lowest temperature (900°C) and the highest strain rate ($10s^{-1}$), increases to 600 MPa for the austenitic steel. Similarly, when the most favorable hot working conditions are applied, i.e. 1000°C and $0.1s^{-1}$, the maximum yield stress curves of about 100 MPa obtained for the duplex steel increase to 200 MPa for the austenitic composition.

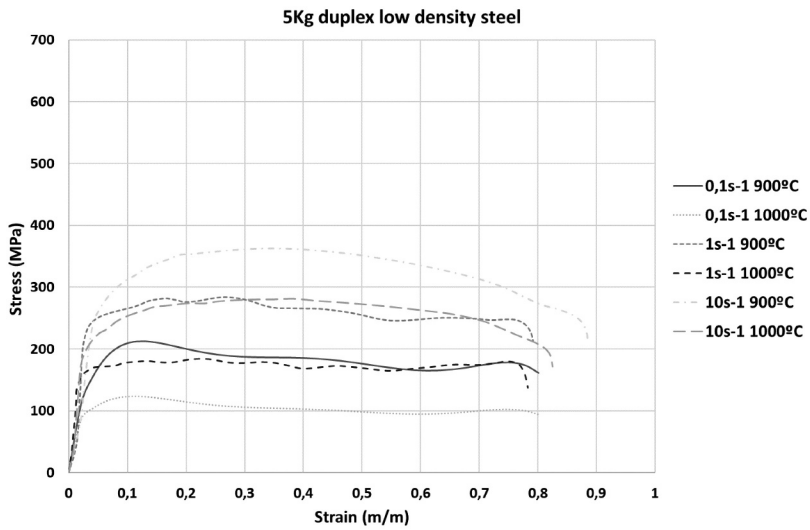

Figure 8. True stress-strain curves of the 5 Kg duplex low-density steel.

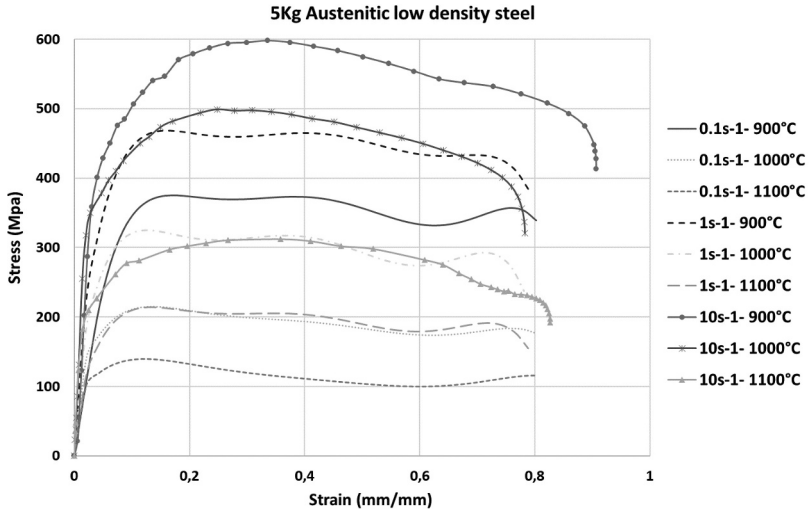

Figure 9. True stress-strain curves of the 5 Kg austenitic low-density steel.

Looking back at the ThermoCalc simulations in Figure 5, in the temperature range used during testing, the ferrite/austenite ratio is approximately 40/60 in the duplex steel and 10/90 in the austenitic steel. During hot working, partitioning of alloying elements carbon, manganese and aluminum occurs between the δ-ferrite and γ-austenite phases. Some transformation of γ to α phase, can also occur at phase boundaries.[23] Due to the partition of the element between two phases, carbon and manganese levels in the austenite are higher than in the ferrite phase as it can be observed in the EDS mapping of the Figure 10, being more pronounced in the case of manganese, whose mapping signal is intensified in austenitic grains. The higher amount of alloying elements in the austenitic steel stabilizes the austenite and increases the strength of the material.

In the 35 Kg duplex low-density steel ingot, a thick slice was cut and compression specimens were machined from the outer and inner parts of the section. The true stress-true strain curves obtained at the same temperatures and strain rates as those used in the prospective tests with the 5 Kg ingots are shown in Figure 11 (inner part of the ingot) and Figure 12 (outer part of the ingot). The flow curves of the material located at the inner and outer parts of the section are quite similar, below 210 MPa the value of the true stress, slight instability at 1100°C and 10 s^{-1}, and mostly steady state without significant recrystallization softening. The flow curve of the test performed at 900°C

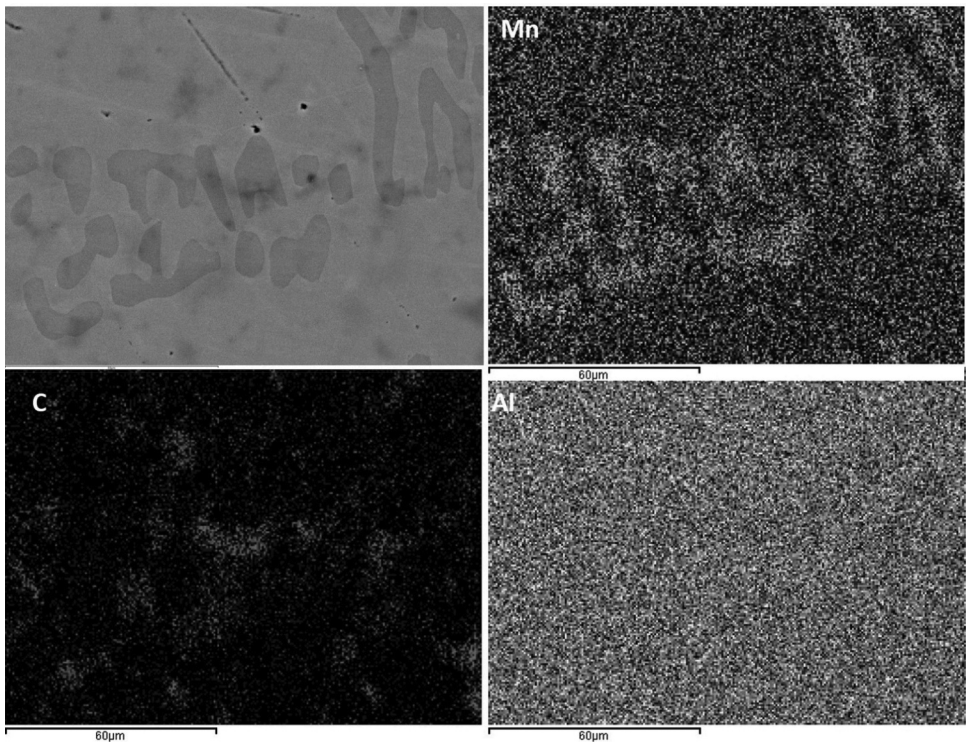

Figure 10. Image obtained by SEM of the 5 Kg duplex low density steel, and the mapping corresponding to the Mn, C and Al alloying elements.

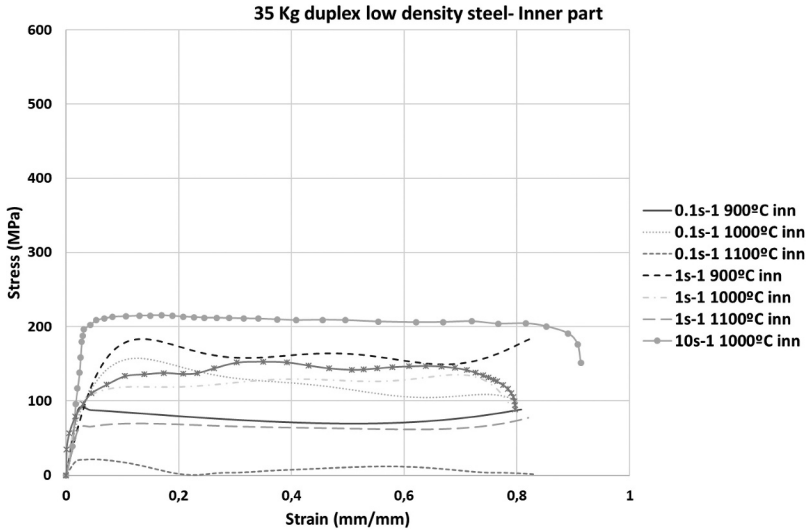

Figure 11. True stress-strain curves of the 35 Kg duplex low-density steel (inner part of the ingot).

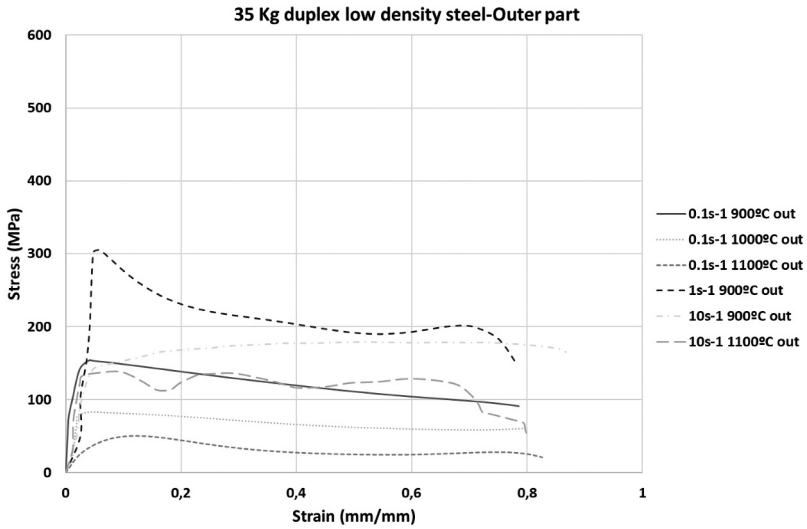

Figure 12. True stress-strain curves of the 35 Kg duplex low-density steel (outer part of the ingot).

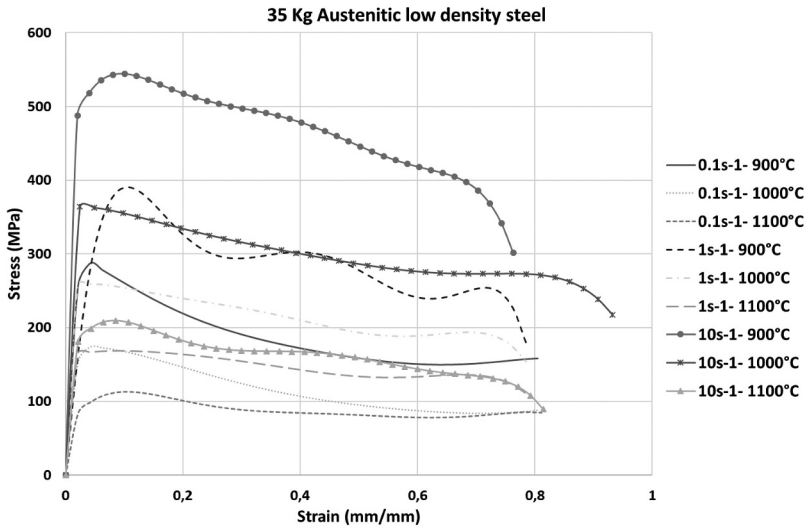

Figure 13. True stress-strain curves of the 35 Kg austenitic low-density steel.

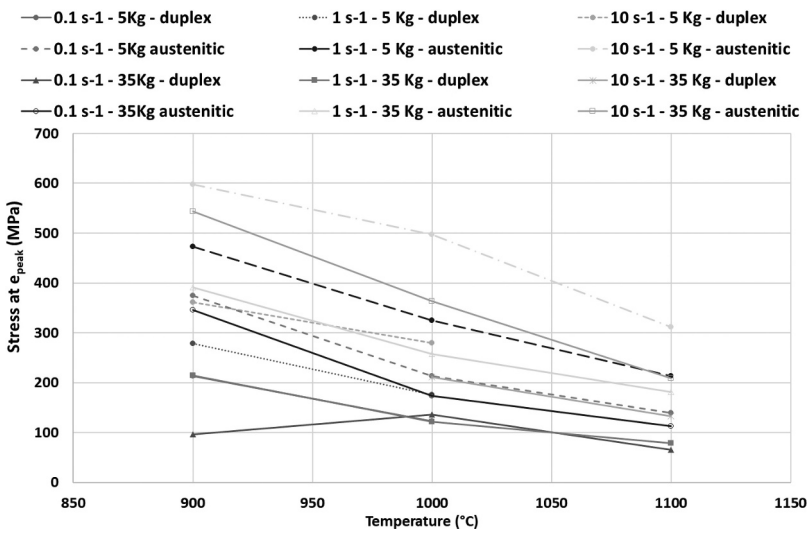

Figure 14. True stress at the peak of strain for 5 Kg and 35 Kg low-density steels.

and $1s^{-1}$ for the outer part shows a remarkable strain hardening with a stress value at the peak of twice the value of all other curves, followed by a dramatic softening. Looking at all the curves together, it is likely that this test probably had an experimental problem, perhaps related to the tantalum layer placed to reduce friction with the anvils. Turning to the curves obtained from specimens machined from the 5Kg duplex steel ingot, the characteristics of the curves are comparable in terms of strain hardening and softening mechanisms although the stress level is lower for the 35 Kg ingot. The very low stress required to compress the material at 1100°C and $0.1s^{-1}$ inside the ingot has no value, which can be the cause of local melting and the the starting point of cracks during the process. For the austenitic material of the 35Kg ingot, the flow curves in Figure 13 are quite different. The stress levels required to compress the specimens are lower than the levels measured for the tests performed on the 5Kg austenitic steel ingot and approximately twice as high as the values obtained for the 35Kg duplex ingot. Furthermore, strain hardening is much more relevant than in the rest of the samples and once the curve crosses the deformation peak, stress decreases similarly (similar gradient) in the tests performed at the highest strain rates. This characteristic may be associated with the dynamic restoration mechanisms that occur during the tests.

It can be assumed that the best conditions for forging would be those for which both the stress and the strain level required to initiate the softening mechanisms are lower. Figures 14 and 15 show the influence of temperature and strain rate on Ɛpeak, the strain value at which dynamic recovery and recrystallization begins in the material, and the stress values at this point. The overall behavior shows a linear decrease of the maximum stress with temperature for a fixed value of strain rate. The stress values of the austenitic steel are higher than those of the duplex steel tested under the same conditions. The values obtained for the specimens machined from the 5Kg ingots are slightly higher than the values obtained for the specimens extracted from the 35Kg ingots. The effect of the test conditions on the Ɛpeak values shows that, in most cases, the minimum value occurs at 1000°C, i.e, recovery and recrystallization start with a lower strain value.Evidence of recrystallization is visible

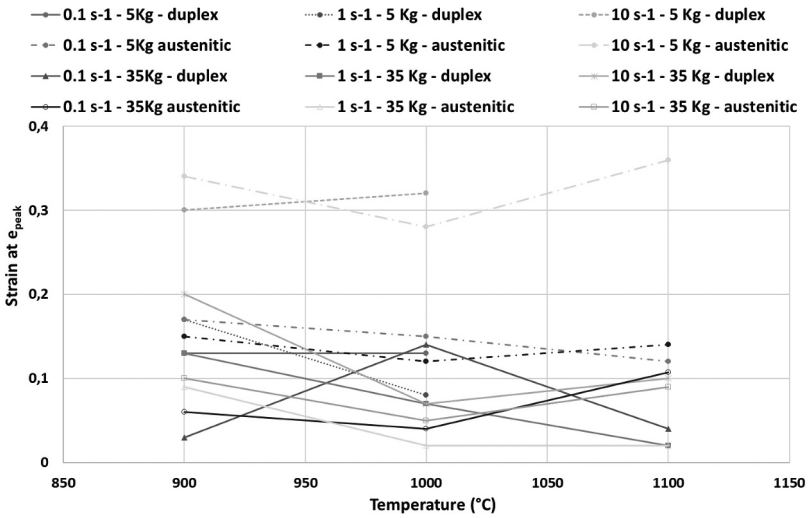

Figure 15. True strain peak for 5 Kg and 35 Kg low-density steels.

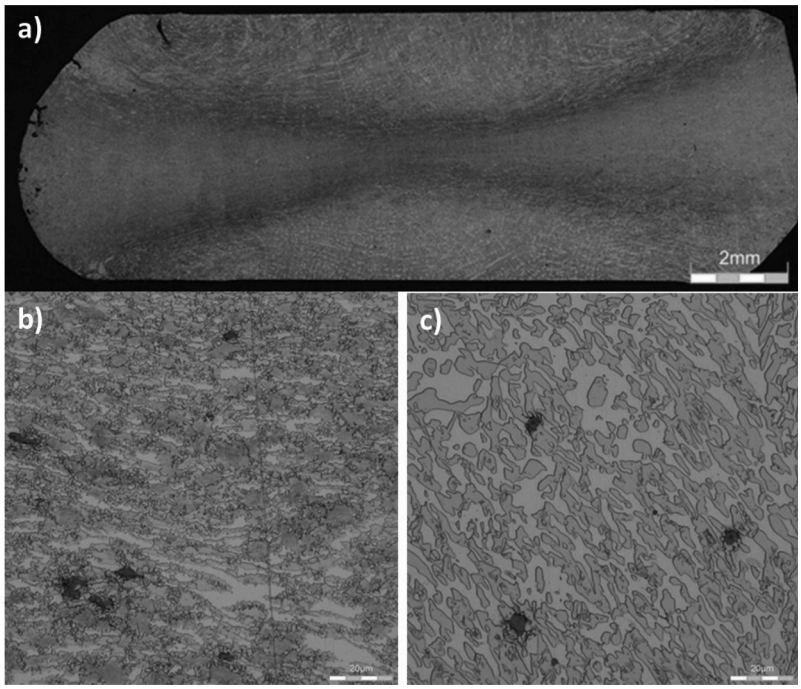

Figure 16. 35 Kg duplex low density steel specimen compressed to a true strain of 0.8. (a) heterogeneous deformation across the section. (b): microstructure of the highly compressed area at the center of the specimen. (c) microstructure of the hardly compressed areas near the specimen-tool contact area.

in the tested samples. Figure 15 shows the cross section of a sample machined from the 35Kg duplex low-density steel. Due to friction with the compression tools, the upper and lower surfaces adhere significantly to the tools, even when there is a sheet of Ta lubricant in-between.Figure 16 The sample deforms heterogeneously, with the maximum deformation in the center of the specimen and minimum in the regions near the top and bottom surfaces. The microstructure of the undeformed area is the expected homogeneous duplex ferrite/austenite. In areas undergoing the highest deformation, small α-ferrite grains recrystallize at phase boundaries, nucleating from the previous δ-ferrite, in good agreement with other authors.[24]

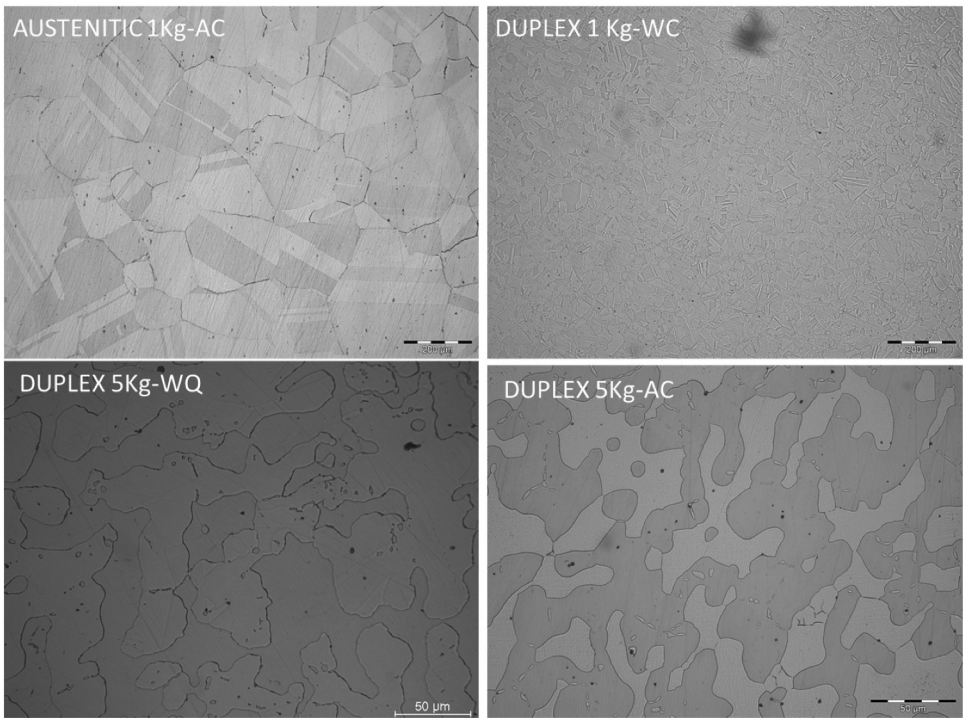

Figure 17. Images obtained by optical microscopy of the microstructures corresponding to the 4 samples subjected to the tensile tests. In the case of the 1 kg samples, the scale bar is 200 micrometers, while in the case of the 5 kg samples, the scale bar is 50 micrometers.

Mechanical properties

Finally, the opportunity to measure the mechanical properties of the two low-density steels successfully forged from castings conducted at different scales was considered. The bars were heated up to 1150°C followed by either air cooling or water quenching. From the bars obtained from the 1Kg and 5Kg ingots, mini-tensile specimens were machined. In the case of the austenitic low-density steel, the yield strength was 1090 MPa and the ultimate tensile strength 1141 MPa, with a total elongation of 37%. In the case of the duplex low-density steel, the best results obtained were 720 MPa and 855MPa for yield strength and ultimate tensile strength respectively, with a total elongations of 22%, in good agreements with other authors.[13,25,26] Figure 17 shows images obtained by optical microscopy of the microstructures corresponding to the 4 samples subjected to the tensile tests. The fully austenitic microstructure of the 1Kg austenitic sample obtained after a normalization heat treatment (heating to 1150°C followed by air cooling), is the microstructure with the best combination of mechanical properties.

Conclusions

The mechanical properties obtained for the low-density steels developed are very promising, also bearing in mind that they can be improved by optimizing the chemical composition and the conditions of the heat treatments. The combination of these properties and the reduction in density of around 15% would allow a significant reduction in the weight of the components and would comply with the lightweighting strategy so much in demand today in many sectors, specially in the automotive industry.

However this requires solving the technological difficulties for their manufacture, which, as has been verified during the course of the research, are very complex. The following conclusions can be drawn from the tests carried out with the different alloys:

- There is a marked scale effect of the ingot. The solidification structure is heterogeneous, and the differences are more pronounced the larger the ingot is because there are greater differences in solidification rate between the core and the surface. This influences the hot mechanical properties and the forgeability of the ingot, making the larger ingots less forgeable and this is more noticeable, the higher the alloying element content.
- The higher the manganese and carbon content, the hot resistance increases and the forgeability deteriorates.
- For all low-density steels, forgeability increases with decreasing the strain rate and increasing forging temperature. Below 900°C, hot resistance increases too much. Above 1100°C there is a risk of segregation of liquid phases at the grain boundary and it is not recommended to prevent the steel from burning and not being forged.
- There is also a very high heat loss due to the high thermal conductivity. The use of refractory dies would be necessary to limit heat loss at low strain rates.

Based on the results obtained, it seems that in order to forge these high aluminum steels correctly, it is necessary to keep the temperature at least above 900°C and below 1100°C, to use a strain rate of less than $1s^{-1}$ and to block heat losses through the dies, e.g. by using refractory dies.

The grades of greatest industrial interest are low-density austenitic steels due to their greater strength, ductility and density reduction potential. However, they are the steels with the worst forgeability and with the most manufacturing problems. Considering the hot forming conditions mentioned above, they could be forgeable, although the heterogeneity of the solidification structure would need to be solved.

Duplex steels are the next option of interest due to their mechanical characteristicsAlthough in theory they are easier to produce than austenitic due to the lower content of alloying elements, it has been shown that the forging precautions mentioned above are also applicable to these grades.

Unfortunately, these low-density steels present considerable difficulties for the usual means of manufacture in industry, both in the steel industry and in metallurgical transformation companies, so their implementation requires special processes and installations.

However, the advantage of these steels in terms of mechanical properties and density reduction could open the door to a sufficiently large market niche to justify an investment in a non-conventional production line specially designed to solve the technological difficulties involved in this type of steels with a high aluminum and manganese content.

Acknowledgments

The authors would like to thank the technical and human support provided by SGIker of UPV/EHU.

Funding

This work was supported by the Basque Government under ELKARTEK Research Program[KK-2016/00029-ABADE] and [KK-2018/00016-COFADEN].

ORCID

Idurre Kaltzakorta http://orcid.org/0000-0001-8459-0287

Conflicts of interest

The authors declare no conflict of interest.

References

[1] Fontaras, G.; Zacharof, N.-G.; Ciuffo, B. Fuel Consumption and CO $_2$ Emissions from Passenger Cars in Europe – Laboratory versus Real-world Emissions. . *Progress in Energy and Combustion Science* 2017, *60*, 97–131. [Web of Science ®], [Google Scholar], [Crossref]. DOI: 10.1016/j.pecs.2016.12.004..

[2] Chen, S.; Rana, R.; Haldar, A.; Ray, R. K. Current State of Fe-Mn-Al-C Low-density Steels. *Prog. Mater. Sci.* 2017, *89*, 345–391. [Web of Science ®], [Google Scholar], [Crossref]. DOI: 10.1016/j.pmatsci.2017.05.002..

[3] Gutierrez-Urrutia, I.;. Low Density Fe–Mn–Al–C Steels: Phase Structures, Mechanisms and Properties. *ISIJ Int.* 2021, *61*(1), 16–25.

[Google Scholar], [Crossref]. DOI: 10.2355/isijinternational.ISIJINT-2020-4..

[4] Chen, D.; Cui, H.; Wang, R. High-Temperature Mechanical Properties of 4.5%Al δ-TRIP Steel [Google Scholar], [Crossref]. *Appl. Sci.*2019, *9*(23), 5094–5102. DOI: 10.3390/app9235094.

[5] Thorat, M. L.; Ligade, R. R. Review on Defects in Hot Forging Process-Investigation. *IJSDR*. 2018, *3*(4), 34–42. [Crossref].

[6] Patel, B. V.; Thakkar, H. R.; Mehta, S. B. Review of Analysis on Forging Defects for Quality Improvement in Forging Industries. *JETIR*. 2014, *1*(7), 871–876. [Google Scholar], [Crossref].

[7] Frommeyer, G.; Brüx, U. Microstructures and Mechanical Properties of High-strength Fe–Mn–Al–C Light-weight Triplex Steels. *Steel Res. Int.* 2006, *77*(9–10), 627–633. [Google Scholar], [Crossref]. DOI: 10.1002/srin.200606440..

[8] Liu, C.; Peng, Q.; Xue, Z.; Wu, T. Research Situation of Fe Mn Al C System Low Density High Strength Steel. *Mater. Rep.* 2019, *33* (15), 2572–2581. [Crossref]. DOI: 10.11896/cldb.18070045..

[9] Rana, R.;. Special Issue on 'Medium Manganese Steels'. *Mater. Sci. Technol.* 2019, *35*(17), 2039–2044. [Taylor & Francis Online], [Google Scholar]. DOI: 10.1080/02670836.2019.1673971..

[10] Rana, R.; Liu, C.; Ray, R. K. Evolution of Microstructure and Mechanical Properties during Thermomechanical Processing of a Low-density Multiphase Steel for Automotive Application. *Acta Mater.* 2014, *75*, 227–245. [Google Scholar], [Crossref]. DOI: 10.1016/j.actamat.2014.04.031..

[11] Raabe, D.; Springer, H.; Gutierrez-Urrutia, I.; Roters, F.; Bausch, M.; Seol, J. B.; Koyama, M.; Choi, P. P.; Tsuzaki, K. Alloy Design, Combinatorial Synthesis, and Microstructure-property Relations for Low-density Fe-Mn-Al-C Austenitic Steels. *JOM*. 2014, *66*(9), 1845–1855. [Web of Science ®], [Google Scholar], [Crossref]. DOI: 10.1007/s11837-014-1032-x..

[12] Gutierrez-Urrutia, I.; Raabe, D. Influence of Al Content and Precipitation State on the Mechanical Behaviour of Austenitic high-Mn Low-density Steels. *Scripta. Mater.* 2013, *68*(6), 343–347. [Web of Science ®], [Google Scholar], [Crossref]. DOI: 10.1016/j.scriptamat.2012.08.038..

[13] Liu, D.; Cai, M.; Ding, H.; Han, D. Control of Inter/intra-granular κ -carbides and Its Influence on Overall Mechanical Properties of a Fe-11Mn-10Al-1.25 C Low Density Steel. *Mat. Sci & Eng. A*, 2018, *715*, 25–32. DOI:10.1016/j.msea.2017.12.102. [Crossref].

[14] Moon, J.; Ha, H.-Y.; Park, S.-J.; Lee, T.-H.; Hang, J. H.; Lee, C.-H.; Han, H. N.; Hong, H.-U. Effect of Mo and Cr Additions on the Microstructure, Mechanical Properties and Pitting Corrosion Resistance of Austenitic Fe-30Mn-10.5Al-1.1C Lightweight Steels. *J. Alloys Compd.* 2019, *775*, 1136–1146. [Crossref]. DOI: 10.1016/j.jallcom.2018.10.253..

[15] Yang, F.; Song, R.; Li, Y.; Sun, T.; Wang, K. Tensile Deformation of Low Density Duplex Fe–Mn–Al–C Steel. *Materials & Design* 2015, *76*, 32–39. [Web of Science ®], [Google Scholar], [Crossref]. DOI: 10.1016/j.matdes.2015.03.043..

[16] Zhang, L.; Song, R.; Zhao, C.; Yang, F.; Xu, Y.; Pen, S. Evolution of the Microstructure and Mechanical Properties of an Austenite-ferrite Fe-Mn-Al-C Steel. *Mat. Sci & Eng. A*. 2015, *643*, 183–193. DOI:10.1016/j.msea.2015.07.043. [Web of Science ®], [Google Scholar], [Crossref].

[17] Rana, R.;. Special Topic: Low Density Steels. *JOM*. 2014, *66*(9), 1730–1733. [Web of Science ®], [Crossref]. DOI: 10.1007/s11837-014-1137-2..

[18] Satya-Prasad, V. V.; Khaple, S.; Baligidad, R. G. Melting, Processing, and Properties of Disordered Fe-Al and Fe-Al-C Based Alloys. *JOM*. 2014, *66*(9), 1785–1793. [Web of Science ®], [Google Scholar], [Crossref]. DOI: 10.1007/s11837-014-1065-1..

[19] Li, Y.-P.; Song, R.-B.; Wen, E.-D.; Yang, F.-Q. Hot Deformation and Dynamic Recrystallization Behavior of Austenite-Based Low-Density Fe–Mn–Al–C Steel. *Acta Metall. Sin. (Engl. Lett.)*. 2016, *29* (5), 441–449. DOI:10.1007/s40195-016-0406-1. [Web of Science ®], [Crossref].

[20] Kim, B.; Jeong, S.; Park, S. J.; Moon, J.; Lee, C. Roles of (Fe, Mn)3Al Precipitates and MBIP on the Hot Ductility Behavior of Fe–30Mn–9Al–0.9C Lightweight Steels. *Met. Mater. Int.* 2019, *25*(4), 1019–1026. DOI: 10.1007/s12540-019-00248-9.. [Web of Science ®], [Crossref].

[21] Yang, F.-Q.; Song, R.-B.; Zhang, L.-F.; Zhao, C. Hot Deformation Behavior of Fe-Mn-Al Light-weight Steel. *Procedia Eng.* 2014, *81*, 456–461. [Web of Science ®], [Crossref] DOI: 10.1016/j.proeng.2014.10.022.

[22] Sozanska-Jedrasik, L.; Mazurkiewicz, J.; Matus, K.; Borek, W. Structure of Fe-Mn-Al-C Steels after Gleeble Simulations and Hot-Rolling. *Mater*. 2020, *13*(3), 739. [Web of Science ®], [Google Scholar], [Crossref]. DOI: 10.3390/ma13030739..

[23] Shin, S. Y.; Lee, H.; Han, S. Y.; Seo, C. H.; Choi, K.; Lee, S.; Kim, N. J.; Kwak, J.-H.; Chin, K.-G. Correlation of Microstructure and Cracking Phenomenon Occurring during Hot Rolling of Lightweight Steel Plates. *Metall. Mater. Trans. A*. 2010, *41*(1), 138–148. DOI: 10.1007/s11661-009-0081-1.. [Web of Science ®], [Google Scholar], [Crossref].

[24] Cai, Z.; Ding, H.; Ying, Z.; Misra, R. D. K. Microstructural Evolution and Deformation Behaviour of a Hot-rolled and Heat Treated Fe-8Mn-4Al-0.2C Steel. *J. Mater. Eng. Perform.* 2014, *23* (4), 1131–1137. [Web of Science ®], [Google Scholar], [Crossref]. DOI: 10.1007/s11665-014-0866-2..

[25] Seol, J. B.; Brief, A. Review of k-Carbide in Fe-Mn-Al-C Model Alloys. *Appl. Microsc*. 2018, *48*(4), 117–121. DOI: 10.9729/AM.2018.48.4.117. [Google Scholar], [Crossref].

[26] Liu, D.; Ding, H.; Cai, M.; Han, D. Mechanical Behaviors of a Lower Mn-added Fe-11Mn-10Al-1.25C Lightweight Steel with Distinguished Microstructural Features. *Mater. Lett.* 2019, *242*, 131–134. [Web of Science ®], [Google Scholar], [Crossref]. DOI: 10.1016/j.matlet.2019.01.115..